THE JOURNAL OF BIOLOGICAL CHEMISTRY VOL. 284, NO. 30, pp. 20249–20262, July 24, 2009

Both Php4 Function and Subcellular Localization Are Regulated by Iron via a Multistep Mechanism Involving the Glutaredoxin Grx4 and the Exportin Crm1*[S]

Received for publication, April 16, 2009, and in revised form, May 21, 2009 Published, JBC Papers in Press, June 5, 2009, DOI 10.1074/jbc.M109.009563

Alexandre Mercier[1] **and Simon Labbé**[1,2]

From the Département de Biochimie, Faculté de Médecine et des Sciences de la Santé, Université de Sherbrooke, Sherbrooke, Quebec J1H 5N4, Canada

In *Schizosaccharomyces pombe*, the CCAAT-binding factor is a multisubunit complex that contains the proteins Php2, Php3, Php4, and Php5. Under low iron conditions, Php4 acts as a negative regulatory subunit of the CCAAT-binding factor and fosters repression of genes encoding iron-using proteins. Under conditions of iron excess, Php4 expression is turned off by the iron-dependent transcriptional repressor Fep1. In this study, we developed a biological system that allows us to unlink iron-dependent behavior of Php4 protein from its transcriptional regulation by Fep1. Microscopic analyses revealed that a functional GFP-Php4 protein accumulates in the nucleus under conditions of iron starvation. Conversely, in cells undergoing a transition from low to high iron, GFP-Php4 is exported from the nucleus to the cytoplasm. We mapped a leucine-rich nuclear export signal that is necessary for nuclear exclusion of Php4. This latter process was blocked by leptomycin B. By using coimmunoprecipitation analysis, we showed that Php4 and Crm1 physically interact with each other. Although we determined that nuclear retention of Php4 *per se* is not sufficient to cause a constitutive repression of iron-using genes, we found that deletion of the *grx4*$^+$-encoded glutaredoxin-4 renders Php4 constitutively active and invariably localized in the nucleus. Further analysis by bimolecular fluorescence complementation assay and by two-hybrid assays showed that Php4 and Grx4 are physically associated *in vivo*. Taken together, our findings indicate that Grx4 and Crm1 are novel components involved in the mechanism by which Php4 is inactivated by iron in a Fep1-independent manner.

Iron is essential to the growth of the vast majority of organisms. Because of its capacity to act as both an electron acceptor and donor, iron has become an indispensable catalytic cofactor for a multitude of enzymes involved in several biological processes ranging from respiration, to the tricarboxylic acid cycle, to DNA synthesis (1). Paradoxically, excess iron is toxic because of its ability to generate hydroxyl radicals via the Fenton chemistry reaction (2). High levels of hydroxyl radicals can produce cellular damage, including direct protein or enzyme inactivation, membrane impairment because of lipid peroxidation, and oxidative DNA damage (3). These two facets of iron require that cells must establish fine-tuned mechanisms to maintain sufficient but not excessive concentrations of iron, thereby keeping the delicate balance between essential and toxic levels of iron.

In *Schizosaccharomyces pombe*, iron homeostasis is controlled by two iron-regulated proteins, the GATA-type transcription factor Fep1 and the CCAAT-binding factor Php4 (4, 5). When iron levels are high, Fep1 binds to GATA *cis*-acting elements found in the promoter regions of genes involved in iron acquisition (*e.g.* *fip1*$^+$, *fio1*$^+$, *frp1*$^+$, and *str1*$^+$/*2*$^+$/*3*$^+$) and shuts down their expression to avoid deleterious consequences of iron overload (6, 7). When iron levels are low, Fep1 is unable to bind DNA, resulting in the transcriptional induction of genes involved in iron acquisition (6, 8, 9). Analogous to *S. pombe*, other fungi use Fep1 orthologs to repress transcription of target genes in response to high iron. Examples include Urbs1 in *Ustilago maydis* (10, 11), SRE in *Neurospora crassa* (12), SreA in *Aspergillus nidulans* (13, 14), Sfu1 in *Candida albicans* (15), and Cir1 in *Cryptococcus neoformans* (16).

In the fission yeast *S. pombe*, one gene that is regulated in a Fep1-dependent manner is *php4*$^+$. *php4*$^+$ encodes a subunit of the CCAAT-binding protein complex, which includes three other subunits, denoted Php2, Php3, and Php5 (17, 18). Genes encoding Php2, Php3, and Php5 are constitutively expressed, whereas transcript levels of *php4*$^+$ are induced under conditions of iron starvation and repressed under iron-replete conditions (18). Php4 is responsible for the transcriptional repression capability of the Php complex and is not required for the DNA binding activity of the complex. A genome-wide microarray analysis revealed that Php4 is capable of coordinating the repression of 86 genes in response to iron starvation (19). Among these genes, several encode proteins involved in iron-dependent metabolic pathways, such as the tricarboxylic acid cycle, mitochondrial respiration, heme biosynthesis, and iron-sulfur cluster assembly. DNA microarray analysis also showed that the gene encoding the iron-responsive transcriptional repressor Fep1 is down-regulated in response to iron deficiency in a Php4-dependent fashion. Based on these data, we proposed a model wherein tight regulation of intracellular iron levels is controlled by the interplay between Php4 and Fep1 through mutual con-

* This work was supported in part by the Natural Sciences and Engineering Research Council of Canada Grant MOP-238238-01 (to S. L.).

[S] The on-line version of this article (available at http://www.jbc.org) contains supplemental Fig. S1.

[1] Recipient of scholarships from the Fonds de la Recherche en Santé du Québec.

[2] To whom correspondence should be addressed: 3001, 12e Ave. Nord, Sherbrooke, Quebec J1H 5N4, Canada. Tel.: 819-820-6868 (Ext. 15460); Fax: 819-

Down-regulation of iron-dependent pathways to optimize the utilization of limited available iron has previously been described in other organisms. When iron is limiting in *Escherichia coli*, the transcriptional repressor Fur is inactivated, leading to increased levels of RyhB, a small noncoding RNA (20). RyhB hybridizes to mRNAs encoding iron-using proteins and triggers their degradation through an RNase E-dependent process (21). In *Saccharomyces cerevisiae*, iron deprivation leads to the activation of the iron-responsive transcription factors Aft1 and Aft2 (22–27). Once activated, these two regulators induce the expression of several genes, including those encoding proteins that function in iron uptake. Additional genes are also positively regulated by Aft1 and Aft2, including *CTH1* and *CTH2*, which encode two CCCH-type zinc finger mRNA-binding proteins that bind AU-rich elements within the 3′-untranslated region of transcripts (28, 29). Among the transcripts that Cth1 and Cth2 can bind and down-regulate in response to iron starvation, several encode iron-using proteins or enzymes that participate in biochemical pathways that use iron as cofactor (29).

As for Aft1 and Aft2, iron-responsive Cth1- and Cth2-like proteins are found mainly in *Saccharomycotina* fungal species (1). The other fungal species such as *Pezizomycotina*, *Taphrinomycotina*, *Basidiomycota*, and *Zygomycota* appear to have a distinct pair of iron-responsive regulatory proteins that include a negative GATA-type transcriptional regulator (*e.g.* Fep1 and SreA) and a negative regulatory subunit of the CCAAT-binding complex (*e.g.* Php4 and HapX) (1).

In *A. nidulans*, a Php4 ortholog, denoted HapX, can trigger down-regulation of genes encoding iron-using proteins during iron deficiency (30). Interestingly, both Php4 and HapX have been shown to be regulated post-translationally by iron (19, 30). Experiments have shown that HapX dissociates from the HapE subunit of the CCAAT-binding complex (HapB-C-E) when iron is abundant (30). Using a one-hybrid approach in fission yeast, a constitutively expressed Gal4-Php4 fusion protein was shown to repress transcription as a function of iron availability when brought to a DNA promoter, revealing that Php4 has the ability to sense iron at the protein level (19). Recent data have provided additional clues with respect to iron sensing. One aspect is the requirement of GSH to allow Php4 to sense iron excess (19). In *S. pombe*, mutant cells defective in GSH biogenesis show markedly decreased transcription of genes encoding iron-using proteins as a result of constitutively active Php4. GSH has also been associated with cellular iron sensing in *S. cerevisiae* (31). As for Php4, Aft1 is constitutively active during GSH deficiency (31). Elegant studies have also determined that *S. cerevisiae* monothiol glutaredoxins Grx3 and Grx4 are key regulators of Aft1 (32, 33). When cells undergo a transition from iron-limiting to iron-sufficient conditions, it has been proposed that Grx3 and Grx4, with the aid of Fra1 and Fra2, transmit an as-yet-unidentified mitochondrial inhibitory signal, which contributes to inactivate Aft1 (32–34).

In this study, we first expressed a functional *GFP-php4*$^+$ allele under the control of a constitutive GATA-less *php4*$^+$ promoter. By use of this system, we ensured that any effects of iron on GFP-Php4 were independent of potential changes in *GFP*

mulated in the nucleus, whereas the protein was exported to the cytoplasm within 60 min of the addition of iron. We identified a functional leucine-rich nuclear export signal (NES)[3] within the region of amino acids 93–100 of Php4. We showed that Php4 binds to Crm1 and is sensitive to leptomycin B (LMB), abolishing its nuclear export behavior. In the presence of LMB, although the GFP-Php4 fusion protein was localized in the nucleus under conditions of both low and high levels of iron, we observed that the protein can still be inactivated by iron, resulting in the derepression of *isa1*$^+$ transcription in response to iron. Deletion of *grx4*$^+$, on the other hand, led to permanent Php4 nuclear accumulation and constitutive repression of *isa1*$^+$. Further analysis by bimolecular fluorescence complementation assay and by two-hybrid assays revealed that Grx4 is a binding partner of Php4. In summary, these results demonstrate that the Php4 subunit of the *S. pombe* CCAAT-binding complex translocates from the nucleus to the cytoplasm in an iron-, Grx4-, and Crm1-dependent manner.

EXPERIMENTAL PROCEDURES

Yeast Strains and Growth Conditions—The *S. pombe* strains used in this study were the wild-type FY435 (*h+ his7-366 leu1-32 ura4-Δ18 ade6-M210*) and four isogenic mutant strains, *fep1Δ* (*h+ his7-366 leu1-32 ura4-Δ18 ade6-M210 fep1Δ::ura4*$^+$), *php4Δ* (*h+ his7-366 leu1-32 ura4-Δ18 ade6-M210 php4Δ::KAN*^{r}), *grx4Δ* (*h+ his7-366 leu1-32 ura4-Δ18 ade6-M210 grx4Δ::KAN*^{r}), and *php4Δ grx4Δ* (*h+ his7-366 leu1-32 ura4-Δ18 ade6-M210 php4Δ::loxP grx4Δ::KAN*^{r}). All five strains were grown in yeast extract medium containing 0.5% yeast extract and 3% glucose that was further supplemented with 225 mg/liter of adenine, histidine, leucine, uracil, and lysine, unless otherwise stated. Strains for which plasmid transformation was required were grown in synthetic Edinburgh minimal medium lacking specific nutrients required for plasmid selection and maintenance. Cells were seeded to an A_{600} of 0.5, grown to exponential phase (A_{600} of ~1.0), and then treated with 250 μM 2,2′-dipyridyl (Dip) or 100 μM $FeSO_4$, or left untreated for 90 min, unless otherwise indicated. *S. pombe grx4Δ* and *php4Δ grx4Δ* disruption strains, as well as control strains, were cultivated in culture jars under microaerobic conditions using the GazPack EZ system (BD Biosciences). For two-hybrid experiments, *S. cerevisiae* strain L40 (*Mat***a** *his3Δ200 trp1-901 leu2-3, 112 ade2 LYS2::*$(lexAop)_4$*-HIS3 URA3::*$(lexAop)_8$*-lacZ*) (35) was grown in synthetic minimal medium containing 83 mg/liter histidine, adenine, uracil, and lysine, 2% dextrose, 50 mM MES buffer (pH 6.1), and 0.67% yeast nitrogen base minus copper and iron (MP Biomedicals, Solon, OH).

Plasmids—The pJK-194*prom*php4*$^+$ plasmid contains a 194-bp DNA segment of the *php4*$^+$ promoter harboring multiple point mutations in the two iron-responsive GATA sequences (positions −188 to −133 and −165 to −160) found

[3] The abbreviations used are: NES, nuclear export signal; BiFC, bimolecular fluorescence complementation; DAPI, 4′,6-diamidino-2-phenylindole; Dip, 2, 2′-dipyridyl; GFP, green fluorescent protein; GSH, glutathione; LMB,

in the *php4*$^+$ promoter (19). The open reading frame (ORF) encoding GFP was PCR-amplified from the pSF-GP1 plasmid (36) and inserted into the SalI and Asp^{718} restriction sites of pJK-194*prom*php4*$^+$ to create pJK-194*prom*php4*$^+$*-GFP*. pJK-194*prom*php4*$^+$*-GFP-php4*$^+$ was constructed through a three-piece ligation by simultaneously introducing a BamHI-SalI PCR-amplified fragment containing the *GFP* gene and a SalI-Asp^{718} PCR-amplified fragment bearing the *php4*$^+$ ORF into a BamHI-Asp^{718}-digested pJK-194*prom*php4*$^+$ plasmid. The *nmt1*$^+$ promoter up to position −1178 from the start codon of the *nmt1*$^+$ gene was amplified by PCR from pREP-41X (37). Once generated, the promoter DNA fragment was inserted into the integrative vector pJK148 (38) at the SacII and BamHI sites. The construct was denoted pJK*nmt*41X. A DNA fragment encoding the *GFP-php4*$^+$ allele was isolated from pJK-194*prom*php4*$^+$*-GFP-php4*$^+$ and then inserted into the BamHI and Asp^{718} restriction sites of pJK*nmt*41X to create pJK*nmt*41X-*GFP-php4*$^+$. To generate the *php4* NES mutant allele (L93A, L94A, L97A, and L100A), the plasmid pJK-194*prom*php4*$^+$*-GFP-php4*$^+$ was used in conjunction with the overlap extension method (39) and the oligonucleotides 5′-CGAGGCAGCTGAGCAGGCAGAGATGGCTCAGGCTC-AGTTGAAGAATTCTACTTTGG-3′ and 5′-GCCTGAGC-CATCTCTGCCTGCTCAGCTGCCTCGTTGTTCTCCT-TCTGTAACTTTCCG-3′ (underlined letters represent nucleotide substitutions that gave rise to mutations) and two oligonucleotides corresponding to the start and stop codons of the ORF of *php4*$^+$. The resulting PCR-amplified fragment was digested with SalI and Asp718 and cloned into pJK*nmt*41X-*GFP*, which was previously engineered by inserting the *GFP* gene into pJK*nmt*41X. The resulting construct was designated pJK-*nmt*41X-*GFP-php4*NESmut. All nucleotide changes were confirmed by DNA sequencing. Plasmids pSP-1178*nmt*-GST-GFP and pSP-1178*nmt*-GST-GFP-Pap1^{515}NES^{533} were constructed by a strategy described previously (40). Plasmid pSP-1178*nmt*-GST-GFP was digested with SpeI and SstI restriction enzymes and used to receive annealed synthetic DNA fragments encoding wild-type and mutant versions of Php4 NES. Resulting plasmids were denoted pSP-1178*nmt*-GST-GFP-Php4^{73}NES^{122} and pSP-1178*nmt*-GST-GFP-Php4^{73}NES^{122}mut, respectively. Plasmid pJK-194*prom*php4*$^+$-TAP-*php4*$^+$ was constructed by replacing the *GFP* ORF in pJK-194*prom*php4*$^+$*-GFP-php4*$^+$ by a PCR-amplified TAP fragment isolated from pREP1-NTAP (41). The purified TAP fragment was also cloned into pJK-194*prom*php4*$^+$ to create pJK-194*prom*php4*$^+$-TAP. Both pJK-194*prom*php4*$^+$-TAP-*php4*$^+$ and pJK-194*prom*php4*$^+$-TAP were subsequently used as templates to subclone their DNA inserts into the pEA500 plasmid (42), creating pEA500-194*prom*php4*$^+$*-TAP-php4*$^+$ and pEA500-194*prom*php4*$^+$*-TAP*, respectively. The *S. pombe crm1*$^+$ promoter up to −1000 from the start codon of the *crm1*$^+$ gene was isolated by PCR and then inserted into the pSP1 vector (43) at the ApaI and PstI sites. The resulting plasmid was denoted pSP1-1000*crm1*$^+$prom. The full-length coding region of *crm1*$^+$ was isolated by PCR, using primers that corresponded to the initiator and stop codons of the ORF. Because the primers contained PstI and XmaI restriction sites, the purified DNA fragment was sites of pSP1-1000*crm1*$^+$prom. The resulting plasmid was named pSP1*crm1*$^+$. The Myc$_{12}$ epitope, obtained from the p*ctr4*$^+$*-X-myc*$_{12}$ plasmid (44) using XmaI and SstI restriction enzymes, was subsequently inserted 3′ to the *crm1*$^+$ gene in pSP1*crm1*$^+$. For two-hybrid interaction assay, the complete or truncated versions of the *php4*$^+$ gene were inserted downstream of and in-frame to the VP16 coding sequence using BamHI and Asp718 restriction sites found in pVP16 (35). The bait plasmid pLexA-*grx4*$^+$ was created by cloning a 747-bp BamHI-PstI DNA fragment containing the full-length coding region of *grx4*$^+$ into the same sites of pLexNA (35).

RNA Isolation and Analysis—Total RNA was extracted by a hot phenol method as described previously (45). RNA samples were quantified spectrophotometrically, and 15 μg of RNA per sample were used for the RNase protection assay, which was carried out as described previously (19). To detect *grx4*$^+$ mRNA levels, plasmid pSK*grx4*$^+$ was created by inserting a 191-bp BamHI-EcoRI fragment from the *grx4*$^+$ gene into the same restriction sites of pBluescript SK (Stratagene, La Jolla, CA). The antisense RNA hybridizes to the region between positions +327 and +518 downstream from the A of the initiator codon of *grx4*$^+$. To generate pSK*VP16*, a 201-bp fragment from the *VP16* gene was amplified and cloned into the BamHI-EcoRI sites of pBluescript SK. Plasmids pSK*isa1*$^+$, pSK*php4*$^+$, and pSK*act1*$^+$ (18) were used to produce antisense RNA probes, allowing the detection of steady-state levels of *isa1*$^+$, *php4*$^+$, and *act1*$^+$ mRNAs, respectively. A riboprobe derived from the plasmid pKS*ACT1* (46) was used to monitor the steady-state levels of *ACT1* mRNAs in experiments using the bakers' yeast strain L40.

Protein Extraction and Immunoblotting—Total cell lysates were prepared as described previously (18). Cell lysates were quantitated using the Bradford assay (47), and equal amounts of each sample were subjected to electrophoresis on 9% SDS-polyacrylamide gels. After electrophoresis, protein samples were electroblotted as described previously (9). The following primary antisera were used for immunodetection: monoclonal anti-GFP antibody (B-2; Santa Cruz Biotechnology) and monoclonal anti-PCNA antibody (PC10; Sigma). After incubation with the primary antibodies, membranes were washed, then incubated with the appropriate horseradish peroxidase-conjugated secondary antibodies (Jackson ImmunoResearch, West Grove, PA), developed with ECL reagents (Amersham Biosciences), and visualized by chemiluminescence.

Fluorescence Microscopy—To analyze the cellular localization of GFP-Php4, an integrative plasmid expressing its corresponding allele under the control of the *php4*$^+$ promoter was transformed into a *php4*Δ strain. Liquid cultures were seeded to an A_{600} of 0.5 and then grown to exponential phase. At log phase (A_{600} of ~1.0), cells were treated with either 250 μM Dip or 100 μM $FeSO_4$. After treatment, direct fluorescence microscopy was conducted as described previously (48). *php4*Δ or *php4*Δ *grx4*Δ cells expressing the wild-type or mutant version of Php4 NES under the control of the *nmt1*$^+$ promoter were precultivated in the presence of thiamine (15 μM) to an A_{600} of ~1.0. At this growth point, cells were washed twice to remove thiamine and seeded to an A_{600} of 0.1 prior to a 16-h incubation

treated 3 h with 250 μM Dip, thereby allowing nuclear targeting of GFP-Php4. At log phase (A_{600} of ~1.0), cells were washed twice to remove Dip and then grown in the presence of 15 μM thiamine to stop *nmt1*$^+$-dependent gene expression. At this point, the nuclear pool of GFP-Php4 was analyzed under conditions of low or high iron for 0, 15, 30, and 60 min. For treatment with LMB (L-2913; Sigma), cells were divided in half and treated with either 100 ng/ml LMB (in 1.4% methanol) or left untreated (with 1.4% methanol as a control), and allowed to continue growing at 30 °C in the presence of 100 μM $FeSO_4$. At relevant time points, aliquots of cells were removed from each half (with or without LMB) and viewed by direct fluorescence microscopy. Cell fields shown in this study are representative of experiments repeated at least five times.

BiFC Analysis—The coding region of VC was amplified by PCR from the template pFA6a-VC-kanMX6 (49) using primers that added unique SalI and Asp718 restriction sites. The PCR product was digested with SalI and Asp718 and cloned into pGEM-7Zf (Promega, Madison, WI). Subsequently, the full-length coding region of *grx4*$^+$ was isolated by PCR and placed in-frame with the VC coding region using the BamHI and SalI restriction sites. The resulting plasmid was designated pGEM-*grx4*$^+$-*VC*. To generate pJK-194*prom*php4*$^+$-*grx4*$^+$-*VC* and pSP1-194*prom*php4*$^+$-*grx4*$^+$-*VC* plasmids, the BamHI-XhoI DNA restriction fragment containing the *grx4*$^+$-*VC* cassette (from plasmid pGEM-*grx4*$^+$-*VC*) was subcloned into the plasmids pJK-194*prom*php4*$^+$ and pSP1-194*prom*php4*$^+$, respectively. The coding regions of *VN* and *php4*$^+$ were generated by PCR amplification with pFA6a-VN-kanMX6 (49) and pJK-194*prom*php4*$^+$-GFP-*php4*$^+$ as templates, respectively. A first pair of primers that incorporates unique 5′ and 3′ BamHI and SalI restriction sites, respectively, was used for *VN*. With respect to *php4*$^+$, we used a set of primers that introduces unique SalI and Asp718 sites at the 5′ and 3′ ends, respectively. The *VN-php4*$^+$ allele was constructed by three-piece ligation by simultaneously introducing the BamHI-SalI PCR-amplified fragment containing VN and the SalI-Asp718 PCR-amplified fragment harboring *php4*$^+$ into the BamHI-Asp718-digested pEA500-194*prom*php4*$^+$ vector. Subsequently, the SacII-Asp718 DNA fragment containing the *VN-php4*$^+$ allele under the control of a GATA-less *php4*$^+$ promoter was cloned into the integrative plasmid pJK210 (38). Microscopic images for BiFC were taken using a magnification of ×1000 with a transmission window at 465–495 nm.

Coimmunoprecipitation—For coimmunoprecipitation experiments, *php4*Δ cells were cotransformed with pEA500-194*prom*php4*$^+$-*TAP* and pSP1-*crm1*$^+$-myc_{12} or pEA500-194*prom*php4*$^+$-*TAP-php4*$^+$ and pSP1-*crm1*$^+$-myc_{12}. Cells were grown to an A_{600} of 0.75 and then incubated in the presence of 250 μM Dip for 3 h. After this growth period, cells were washed twice and then re-incubated in the presence of 100 μM $FeSO_4$ for 15 min. Total cell lysates were obtained by glass bead disruption in lysis buffer (10 mM Tris-HCl (pH 7.9), 0.1% Triton X-100, 0.5 mM EDTA, 20% glycerol, 100 mM NaCl, 1 mM phenylmethylsulfonyl fluoride) containing a mixture of protease inhibitors (P-8340; Sigma). Typically, 8–10 mg of total protein were added to a 15-μl bed volume of IgG-Sepharose 6 Fast-30 min at 4 °C. Beads were washed four times with 1 ml of lysis buffer, with the beads transferred to a fresh microtube before the last wash. The immunoprecipitates were resuspended in 60 μl of SDS loading buffer, incubated for 5 min at 95 °C, and resolved by electrophoresis on a 9% SDS-polyacrylamide gel. For protein analysis of Crm1-myc_{12}, TAP-Php4, and PCNA, the following primary antisera were used: monoclonal anti-Myc antibody 9E10 (Roche Applied Science); polyclonal anti-mouse IgG antibody (ICN Biomedicals, Aurora, OH); and monoclonal anti-PCNA antibody PC10 (Sigma).

Two-hybrid Analysis—Pre-cultures of each L40 cotransformant strain harboring the indicated bait and prey plasmids were grown to an A_{600} of 0.5. Samples were withdrawn from the cultures, and quantitative measurements of β-galactosidase activity were assayed using buffers and the substrate *o*-nitrophenyl-β-D-galactopyranoside as described previously (50). Levels of β-galactosidase activity were measured within the linear response range and expressed in standard units (51). Values shown are the average of triplicate assays of three independent cotransformants. For protein expression analysis, the antibodies used were the monoclonal anti-LexA 2-12 directed against the LexA DNA binding domain and anti-VP16 1-21 directed against the VP16 activation domain (both from Santa Cruz Biotechnology). A monoclonal anti-3-phosphoglycerate kinase antibody (Molecular Probes, Eugene, OR) was used to detect the phosphoglycerate kinase protein as an internal control.

RESULTS

Inactivation of Php4 by a Fep1-independent Mechanism—As we have previously shown (18, 19) inactivation of Php4 in response to iron is regulated at two distinct levels. First, in the presence of iron, Fep1 associates with GATA elements in the *php4*$^+$ promoter to repress transcription, ensuring the extinction of most *php4*$^+$ transcripts. Second, we observed that in the absence of Fep1, although *php4*$^+$ mRNA levels are constitutive and unresponsive to iron for repression, the gene product (Php4) can still be inactivated by iron. Iron-mediated inhibition of Php4 results in transcriptional induction of the regulon of genes controlled by Php4 (19). To begin to characterize the mechanism by which Php4 activity is regulated by iron in a Fep1-independent manner, we developed a biological system in which *php4*$^+$ and *GFP-php4*$^+$ alleles were expressed under the control of a GATA-less *php4*$^+$ promoter. By use of this system, we determined that *php4*Δ mutant cells expressing *php4*$^+$ or *GFP-php4*$^+$ exhibited *php4*$^+$ mRNA levels that were constitutively expressed under both low and high iron concentrations (Fig. 1*A*). As control for normal transcriptional regulation, the steady-state levels of *php4*$^+$ were down-regulated when wild-type cells were grown under basal and iron-replete conditions (Fig. 1*A*, *WT*). As controls for signal specificity, cells harboring an inactivated *fep1*$^+$ gene (*fep1*Δ) exhibited a constitutive transcription of *php4*$^+$, and *php4*$^+$ mRNA was absent in *php4*Δ null cells (Fig. 1*A*). Subsequently, we examined the effect of a sustained *php4*$^+$ or *GFP-php4*$^+$ expression on the transcriptional profile of *isa1*$^+$, a Php4-regulated target gene (Fig. 1*B*). When Php4 was constitutively expressed, we observed that the repres-

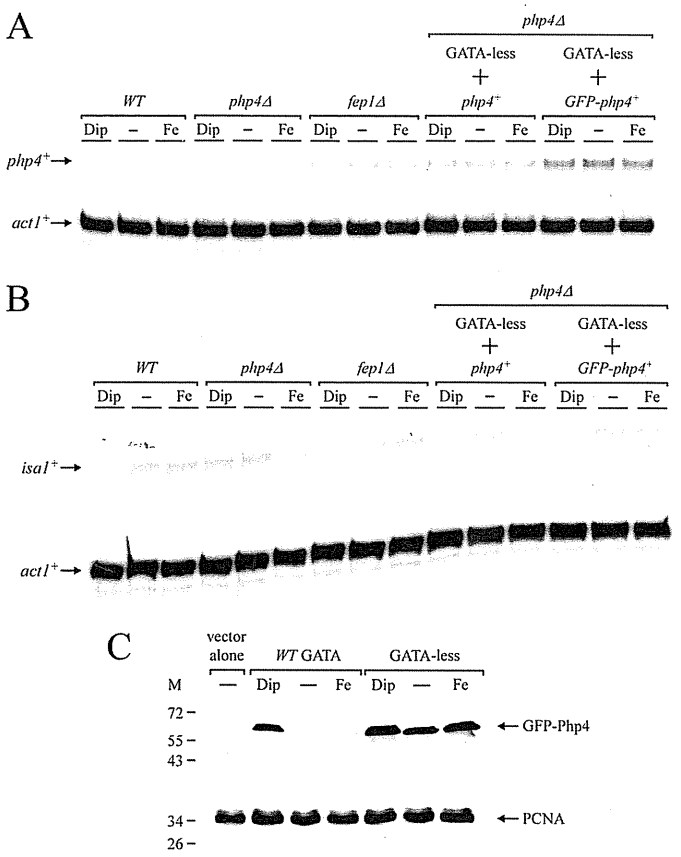

FIGURE 1. **Php4 is inactivated in a Fep1-independent manner.** *A*, logarithmic phase cultures of isogenic strains FY435 (*WT*), AMY15 (*php4*Δ), and BPY10 (*fep1*Δ) were untreated (−) or treated in the presence of Dip (250 μM) or $FeSO_4$ (Fe) (100 μM) for 90 min. After treatment, total RNA was prepared from each sample and analyzed by RNase protection assays. Steady-state levels of *php4*$^+$ and *act1*$^+$ mRNAs (indicated with *arrows*) were analyzed in the wild-type strain and strains lacking the *php4*$^+$ or *fep1*$^+$ allele. When indicated, *php4*Δ cells were transformed with the integrative plasmids pJK-194*prom*php4*$^+$-*php4*$^+$ (*GATA-less* + *php4*$^+$) and pJK-194*prom*php4*$^+$-*GFP-php4*$^+$ (*GATA-less* + *GFP-php4*$^+$). *B*, aliquots of the cultures described for *A* were examined by RNase protection assays for steady-state levels of *isa1*$^+$ mRNA. The *arrows* indicate signals corresponding to *isa1*$^+$ and *act1*$^+$ transcripts. RNase protection data shown in *A* and *B* are representative of three independent experiments. *C*, cells carrying a disrupted *php4*Δ allele were transformed with an empty plasmid (*vector alone*), or plasmids expressing *GFP-php4*$^+$ under the control of the wild-type *php4*$^+$ promoter (*WT GATA*), or under the regulation of a GATA-less *php4*$^+$ promoter (*GATA-less*). Transformed cells were grown under basal (−) or iron-deficient conditions (250 μM Dip) or with excess iron (100 μM $FeSO_4$) (*Fe*). Whole-cell extracts were prepared and analyzed by immunoblotting with anti-GFP or anti-PCNA (as an internal control) antibody. *M*, the positions of the molecular weight standards are indicated to the *left*.

that in the absence of Fep1 or its iron-responsive *cis*-acting elements iron can still trigger the inactivation of Php4 (Fig. 1*B*).

To ensure that fusion of GFP to the N terminus of Php4 did not interfere with its function, we analyzed if iron limitation-dependent down-regulation of *isa1*$^+$ gene expression was corrected by integrating a *GFP-php4*$^+$ allele expressed from both the wild-type *php4*$^+$ promoter (data not shown) and its derivative version containing mutated GATA elements. As shown in Fig. 1*B*, *GFP-php4*$^+$ repressed *isa1*$^+$ mRNA levels under iron-limiting conditions in a manner similar to that of the wild-type *php4*$^+$ allele. Furthermore, the ability of GFP-Php4 to repress *isa1*$^+$ transcript levels occurred with both types of *php4*$^+$ promoter, native and GATA-less. To further investigate the effect

Php4 (predicted mass of 59.8 kDa) when expressed under the control of the GATA-less promoter. Immunoblot analyses revealed that GFP-Php4 is stable and present in similar relative amounts in iron-deficient and iron-replete cells, suggesting that the mechanism of Php4 inactivation was not operated through iron-regulated changes in protein synthesis or stability (Fig. 1*C*). On the other hand, we observed that steady-state levels of GFP-Php4 were dramatically reduced in cells grown in the presence of iron (or left untreated) when the fusion allele was under the control of the wild-type *php4*$^+$ promoter (Fig. 1*C*). Therefore, despite a constitutively expressed GFP-Php4, either from a *fep1*Δ strain or a GATA-less promoter, the Php4 target gene *isa1*$^+$ was only repressed under low iron conditions. These results strongly suggest that iron can trigger the inactivation of Php4 function through an additional mechanism that is independent of Fep1-mediated transcriptional repression.

Iron Starvation Induces Nuclear Accumulation of GFP-Php4—To further investigate the mechanism by which Php4 activity is regulated, we examined the localization of Php4 in response to changes in iron levels. To perform these experiments, we used a *php4*Δ mutant strain where expression of the *GFP-php4*$^+$ allele was under the control of a GATA-less *php4*$^+$ promoter. Cells were grown in minimal medium (under basal conditions) to exponential phase and then treated with the iron chelator Dip (250 μM) or $FeSO_4$ (100 μM) for 3 h. Following treatment with Dip, GFP-Php4 localized to the nucleus (Fig. 2). Consistent with this observation, GFP-Php4 fluorescence colocalized with the DNA-staining dye DAPI, which was used as a marker for nuclear staining. When cells were treated with $FeSO_4$, GFP-Php4 was viewed primarily in the cytoplasm (Fig. 2). Before treatment (at the zero time point; minimal medium contained 74 nM iron), GFP-Php4 displayed a pancellular-fluorescence pattern (Fig. 2). As we observed previously, GFP alone was cytoplasmic as well as nuclear (52). Taken together, these results indicate that GFP-Php4 localizes to the nucleus in iron-deficient cells but is detected in the cytoplasm when cells are grown under iron-replete conditions.

The nuclear accumulation of GFP-Php4 in response to iron starvation prompted us to examine the fate of the nuclear pool of Php4 in response to variations in iron levels. To address this point, we used the *nmt1*$^+$-inducible/repressible promoter system (53). Expression of an integrated *GFP-php4*$^+$ allele under the control of the *nmt1*$^+$ 41X promoter (37) allowed us to induce the synthesis of GFP-Php4 in the presence of Dip, thereby fostering its nuclear sequestration (Fig. 3*A*). Prior to *nmt1*$^+$ transcriptional shut-off, basal levels of *GFP-php4*$^+$ mRNA were detected in *php4*Δ cells (Fig. 3*B*, T_0). Under the same low iron and thiamine-free conditions, we observed that GFP-Php4 localized in the nucleus (Fig. 3*A*, T_0). After the addition of thiamine to repress further synthesis (Fig. 3*B*), we examined the effects of iron, manganese, cobalt, and Dip on the subcellular localization of GFP-Php4. As shown in Fig. 3*A*, when cells were incubated for 60 min with 100 μM $FeSO_4$, GFP-Php4 was exported from the nucleus to the cytoplasm. In contrast, when cells were treated with $MnCl_2$ (100 μM), $CoCl_2$ (100 μM), or Dip (250 μM), there was no apparent change in the localization of GFP-Php4, with its fluorescent signal observed primarily

DOCKET ALARM

Explore Litigation Insights

Docket Alarm provides insights to develop a more informed litigation strategy and the peace of mind of knowing you're on top of things.

Real-Time Litigation Alerts

Keep your litigation team up-to-date with **real-time alerts** and advanced team management tools built for the enterprise, all while greatly reducing PACER spend.

Our comprehensive service means we can handle Federal, State, and Administrative courts across the country.

Advanced Docket Research

With over 230 million records, Docket Alarm's cloud-native docket research platform finds what other services can't. Coverage includes Federal, State, plus PTAB, TTAB, ITC and NLRB decisions, all in one place.

Identify arguments that have been successful in the past with full text, pinpoint searching. Link to case law cited within any court document via Fastcase.

Analytics At Your Fingertips

Learn what happened the last time a particular judge, opposing counsel or company faced cases similar to yours.

Advanced out-of-the-box PTAB and TTAB analytics are always at your fingertips.

API

Docket Alarm offers a powerful API (application programming interface) to developers that want to integrate case filings into their apps.

LAW FIRMS
Build custom dashboards for your attorneys and clients with live data direct from the court.

Automate many repetitive legal tasks like conflict checks, document management, and marketing.

FINANCIAL INSTITUTIONS
Litigation and bankruptcy checks for companies and debtors.

E-DISCOVERY AND LEGAL VENDORS
Sync your system to PACER to automate legal marketing.